Hox clusters of the bichir (Actinopterygii, *Polypterus senegalus*) highlight unique patterns of sequence evolution in gnathostome phylogeny

Jeremy D. Raincrow[1], Ken Dewar[2], Li-Zhi Gao[1], Claudia Stocsits[3], Sonja J. Prohaska[3,4], Ken Dewar[5], Chris T. Amemiya[6,7], Peter F. Stadler[3,4,5,8], Chi-hua Chiu[1*]

[1]Department of Genetics, Rutgers University, 145 Bevier Road, Piscataway, NJ 08854, USA

[2]McGill University and Genome Quebec Innovation Centre, 740 Avenue Doctor-Penfield, Montreal, Quebec HCA 1A4, Canada

[3]Department of Theoretical Chemistry, University of Vienna, Wahringerstrasse 17, A-1090 Wien, Austria

[4]Bioinformatics Group, Department of Computer Science, Interdisciplinary Center for Bioinformatics, University of Leipzig, Hartelstrasse 16-18, D-04107 Leipzig, Germany

[5]McGill University and Genome Quebec Innovation Centre, 740 Avenue Doctor-Penfield, Montreal, Quebec H3A 1A4, Canada

[6]Benaroya Research Institute at Virginia Mason, 1201 Ninth Avenue, Seattle, WA 98101, USA

[7]Department of Biology, University of Washington, 106 Kincaid Hall, Seattle, WA 98185, USA

[8]Santa Fe Institute, 1399 Hyde Park Road, Santa Fe, NJ 87501, USA

*Corresponding author

Chi-hua Chiu
Department of Genetics, LSB Rm. 222
Rutgers University
145 Bevier Road
Piscataway, NJ 08854
732-445-2563 (office); 5-1147 (fax)
chiu@biology.rutgers.edu

ABSTRACT

The *Hox* gene complex of gnathostomes represents a highly constrained genetic system. The nature of this constraint, however, remains poorly understood. Evidence from shark, coelacanth, and tetrapods supports that two rounds of whole genome duplications lead to four clusters (*Hox*A, *Hox*B, *Hox*C, *Hox*D) in the jawed vertebrate ancestor. They exhibit a striking degree of conservation in cluster architecture and intergenic noncoding sequences. A third duplication occurred in the crown group of teleosts producing up to eight *Hox* clusters. The duplicated *Hox* clusters of teleosts show dynamic changes in architecture and accelerated rates of evolution in both protein-coding and noncoding sequences, rendering comparisons to outgroup taxa such as human or shark challenging. Using independent strategies including BAC library screening, homeobox PCR surveys, phylogenetic analyses, and examination of patterns of conservation of noncoding sequences we provide conclusive evidence that the bichir (*Polypterus senegalus*) has four *Hox* clusters that are orthologous to those of the ancestral gnathostome. Detailed analyses of patterns of conservation of *Hox* noncoding sequences and invasions of repetitive and mobile DNA sequence elements into *Hox* clusters of bichir and teleosts highlights a trend towards relaxation of selective constraints acting on actinopterygian *Hox* clusters that --- surprisingly --- predates the fish specific genome duplication.

Keywords: Hox, *Polypterus senegalus*, phylogenetic footprinting

INTRODUCTION

Hox genes encode a distinct class of transcription factors that play an essential role in embryonic patterning (Lewis, 1978; McGinnis and Krumlauf, 1992) and are components of the strikingly conserved genetic toolkit responsible for the diversity of body plans (Gehring, 1998). Present evidence suggests that *Hox* genes originated after the divergence of sponge and eumetazoan lineages, coinciding with a major evolutionary transition in animal body-plan complexity (Larroux et al., 2007). With a few notable exceptions such as nematode (*Caenorhabditis elegans*, Aboobaker and Blaxter, 2003), tunicate (*Oikopleura dioica*, Seo et al., 2004), and platyhelminth (*Schistosoma mansoni*, Pierce et al., 2005), *Hox* genes tend to occur in tightly linked clusters. These display the phenomenon of colinearity, in which the position of a gene in the cluster is related to its spatiotemporal pattern of expression along the anteriorposterior (A-P) axis (McGinnis and Krumlauf, 1992; Lufkin, 1996). It is important to note, however, that the emergence of *Hox* spatial and temporal colinearity during evolution remains poorly understood (Galliot, 2005; Monteiro and Ferrier, 2006). Additionally, a proper spatial expression is observed in several species where *Hox* clustering is absent (Kmita and Duboule, 2003).

Protostome taxa possess at most a single *Hox* cluster. As illustrated in Figure 1, the vertebrate *Hox* gene family expanded via whole cluster duplications (Meyer and Schartl, 1999; Ruddle et al. 1999). Present knowledge suggests that jawless vertebrates (agnathans) such as hagfish (Stadler et al., 2004) and lamprey (Force et al., 2002; Irvine et al., 2002; Fried et al., 2003; Prohaska et al., 2006) have at least three *Hox* clusters, some or all of which may have originated from lineage specific duplications. Among the jawed vertebrates (gnathostomes, Figure 1), cartilaginous fishes such as the elephant shark (*Callorhinchus milii*, Venkatesh et al.,

2007), and horn shark (*Heterodontus franciscii*, Kim et al., 2000; Prohaska et al., 2004) possess four Hox clusters orthologous to the A,B,C,D clusters shared by the lobe-finned fishes, i.e. tetrapods (Ruddle et al., 1994) and coelacanth (*Latimera menadoensis*, Koh et al., 2003), and lungfish (*Neoceratodus forsteri*, Longhurst and Joss, 1999). Remarkably, *Hox* cis-regulatory sequences are conserved between horn shark and human (Chiu et al., 2002; 2004; Prohaska et al., 2004), suggesting strong selective constraints acting on gnathostome *Hox* cluster architecture and regulation throughout their evolution. In stark contrast, however, investigations on *Hox* sequence evolution in the ray-finned fishes, the third major gnathostome clade, demonstrate a unique plasticity (Chiu et al., 2004; Brunet et al., 2006).

There are more than 23,000 extant actinopterygian species (Nelson, 1994) and, judging by the degree of anatomical diversity, this lineage may be considered to be the most successful of all vertebrates (Carroll, 1988). As illustrated in Figure 1, the ray-finned fish lineage experienced a third round of whole genome duplication (Taylor et al., 2003; Jaillon et al., 2004; Woods et al., 2005; Brunet et al., 2006; Kasahara et al., 2007) in the crown group of teleosts circa 350 million years ago (Taylor et al., 2001; Christoffels et al., 2004; Vandepoele et al., 2004). As a result of this Fish Specific Genome Duplication (FSGD), teleost fishes are the pinnacle of *Hox* cluster evolution, with linkage evidence for eight *Hox* clusters in zebrafish (*Danio rerio*, Amores et al., 1998; Woltering and Duston, 2006), and seven in pufferfishes (*Takifugu rubripes*, Aparicio et al., 2002; Amores et al,. 2004 and *Tetraodon nigrividis*, Jaillon et al., 2004), medaka (*Oryzias latipes*, Naruse et al., 2000; Kurosawa et al., 2006; Kasahara et al., 2007), and African cichlid (*Astatotilapia burtoni*, Hoegg et al., 2007).

Chiu et al., (2004) sequenced the single *Hox*A cluster of bichir and showed it is mosaic in its patterns of conservation of noncoding sequences, effectively bridging outgroup taxa (e.g.

shark, coelacanth, human) and teleosts that possess duplicate *Hox* clusters as a result of the FSGD. In this study we show that bichir has single *Hox*A, B, C, and D clusters using a combination of methods. Similarly to the bichir *Hox*A cluster (Chiu et al., 2004), the *Hox*B, C, and D noncoding sequences also show a mosaic pattern, bridging outgroups and teleost fishes. We show here that the *Hox* clusters of bichir have been invaded by repetitive and mobile DNA elements in a pattern that continued to expand in teleosts. This suggests that active DNA transposition into *Hox* clusters may serve an important, presently unrecognized, role in actinopterygian *Hox* cluster evolution. Taken together, our findings suggest an evolutionary trend towards relaxation of selective constraints acting on actinopterygians *Hox* clusters occurred in the stem lineages prior to the fish specific duplication. This study provides important insights into the genomic contributions of actinopterygian phenotypic diversity.

MATERIALS AND METHODS

Isolation and assembly of bichir (Polypterus senegalus) Hox clusters

Details of the bichir (*Polyterus senegalus*) BAC genomic library as well as the isolation and sequencing of the *Hox*A cluster are provided in Chiu et al., (2004). In general, we screened the library by either (1) hybridization of the 5 x 5 high density filters (Chiu et al., 2004) and/or (2) a combination of PCR screening of DNA pools (1 pool = 384 clones; 216 total pools) of the BAC library and hybridization of a small 'pool specific' filter (384 spots). Hybridization using non-radioactive DIG-labeled probes was done following methods described in (Chiu et al., 2000). The first screen of this library was carried out using a pool of homeobox sequences isolated in genome-wide PCR surveys from bichir (Ledje et al., 2002) and coelacanth. This screen identified four BAC clones of *P. senegalus*. A PCR survey of each BAC clone was done using a degenerate homebox primer pair [334, `5′-GAR YTI GAR AAR GAR TTY-3′`; 335, `5′-ICK ICK RTT YTG RAA CAA-3′`]. One clone contained a portion of the *Hox*A cluster (Chiu et al. 2004); one contained the related ParaHox cluster (Mulley et al., 2006); one contained part of the *Hox*B cluster (*Hox*B9 and *Hox*B10), and the last clone contained part of the *Hox*D cluster (*Hox*D2 and *Hox*D3).

To find an overlapping *Hox*B clone, we designed PCR primers specific to bichir *Hox*B10 exon 1 […..] and PCR screened the library; this identified clone (**181G24**), which spans *Hox*B13-*Hox*B4 (Figure 2). Using degenerate primers [….], we amplified *Hox*B2 from bichir whole genomic DNA, designed bichir HoxB2 specific primers [….], and then PCR screened the BAC library pools. This yielded clone (**192O14**), which contains *Hox*B1 and *Hox*B2 (Figure 2). To find overlapping *Hox*D clones, we amplified *evx*2 from bichir whole genomic DNA using

degenerate primers […], designed bichir specific *evx*2 primers […], and subsequently PCR screened the BAC library. This yielded one clone (**20M19**), which contains *evx*2 and *Hox*D12. Using degenerate *Hox*D9 primers […], we isolated the bichir *Hox*D9 gene proper region (Figures 2, 3). PCR screening of the BAC library pools with bichir specific *Hox*D9 primers and hybridization of the high density filters failed to find a BAC clone. Using primers specific for bichir *Hox*D3 […], we PCR screened the library pools and isolated a second clone (**184C8**) that spans *Hox*D3-*Hox*D1. BAC clone sequences have been deposited into Genbank with accession nos. (X).

Hox Cluster Sequences

Hox cluster sequences from a variety of sources were used in this study.

Polypterus senegalus: *Hox*A= ***AC126321*** and ***AC132195*** as in (Chiu et al., 2004). The partial *Hox*B cluster is constructed from the draft sequence of clone L28995 (accession number ***AC138147***): *Hox*B13 is located on segment L28995.23, *Hox*B10 on L28995.7, *Hox*B8 and *Hox*B7 on L28995.17, *Hox*B5 and *Hox*B4 are on segment L28995.1. The finished sequence of clone CLN84 contains *Hox*D3, *Hox*D2, and *Hox*D1. The finished sequence of M19 contains *Hox*D12 and evx2.

Homo sapiens: *Hox*A was combined from clones with Genbank accession numbers ***AC004079***, ***AC004080,*** and ***AC010990*** as described in (Chiu et al., 2002). The other three clusters were excised from the May 2004, Build 35, of the human genome, downloaded from the UCSC genome browser (http://genome.ucsc.edu): *Hox*B = Chr.17: 43,961,813-44,161,040; *Hox*C = Chr.12: 52,618,296-52,735,253; *Hox*D = Chr.2: 176,772,385-176,881,142.

Xenopus tropicalis: Assembly JGI3 release obtained from ENSEMBL (http://www.ensembl.org) release 36.1b: *Hox*A = scaff.29: 1,777,789-2,133,531; *Hox*B =

scaff.329: 415,000-1,016,000; *Hox*C = scaff.280: 199,492-581,365; HoxD = scaff.353: 474,676-800,000.

Heterodontus francisci: *Hox*A is a composite of ***AF479755*** and ***AF224262***, *Hox*D = ***AF224263*** (Kim et al., 2000).

Danio rerio: *Hox*Aa = ***AC107364*** with several modifications including trimming the first 26,896 and the last 4,176 nucleotides and inserting a C at position 76,071. *Hox*Ab = ***AC107365*** with nucleotide 79,324 changed from T to C to avoid a premature stop codon. *Hox*Ba = ***BX297395*** and ***AL645782***, which overlap in the *Hox*B4a locus. HoxBb = ***AL645798.*** *Hox*Ca = ***BX465864*** and ***BX005254***. *Hox*Cb is extracted from the assembly Zv5, ENSEMBL release 31.4d.

*Hox*Da = ***BX322661.***

*Oreochromis niloticus: Hox*A = ***AF533976.***

Morone saxatilis: *Hox*A= ***AF089743.***

Oryzias latipes: ***AB232918-Ab232924***

Tetraodon nigroviridis: sequences were retrieved from the Tetraodon Genome Browser (http://www.genoscope.cns.fr/externe/tetranew/entry_ggb.html), Aug 2005. *Hox*Aa = Chr.21: 2,878,001-3,153,406; *Hox*Ab = Chr.8: 6,506,471-6,727,504; *Hox*Ba = Un: 37,928,410-38,293,032; *Hox*Bb = Chr.2: 1,321,876-1,537,033; *Hox*Ca = Chr.9: 4,083,941-4,353,227; *Hox*Da = Chr.2: 10,975,763-11,218,409, with deleting a T at position 11,134,740 to stay in frame; HoxDb = Chr.17: 9,471,355-9,694,740.

Takifugu rubripes}: sequences were downloaded from the Ensembl genome browser (assembly FUGU 2.0). The *Hox*Aa cluster isconstructed from the entire scaffold 47, the *Hox*Ab} cluster is constructed from scaffold 330 (Chiu et al., 2002).

Latimeria menadoensis Hox clusters will be described in detail in Powers et al (2009). Genbank Accession numbers xxxx.

The sequences will become available in Genbank in the next weeks, I will submit them next week as part of preparing the following paper.
Characterization of the HOX cluster sequences in the basal sarcopterygian *Latimeria menadoensis*, Thomas P. Powers, Jane Grimwood, Jeremy Schmutz, Mark Dickson, Tsutomu
Miyake, Sonja Prohaska, Gunter P. Wagner, Richard M. Myers, Francis H.
Ruddle, Peter Stadler, and Chris T. Amemiya, 2009, in preparation)

Phylogenetic analysis supports bichir has four Hox clusters

Alignments of *Hox* gene predicted amino acid sequences were done using the clustalW algorithm in the software package MacVector version 8.1.1 using default settings. Amino acid alignments were corrected by eye and trimmed so each sequence was of equal length.

Maximum Parsimony trees were created using PAUP* v4.0b10 (Swofford 2003) under the parsimony optimality criterion. Heuristic searches were performed under default settings. Node confidence was scored using the bootstrap resampling method with 2000 replicates and 50% cutoff. Neighbor-Joining trees were created using PAUP* v4.0b10 under the distance optimality criterion using default settings. Node confidence was scored using the bootstrap resampling method with 2000 replicates and 50% cutoff. Maximum Likelihood trees were obtained using GARLI v0.951 (Zwick 2006), which can be downloaded from http://www.bio.utexas.edu/faculty/antisense/garli/Garli.html. Default settings were used unless otherwise stated below. Starting trees were obtained using heuristic search under the likelihood optimality criterion in PAUP* v4.0b10, default settings were used. The substitution model was set to the 2 rate model which corresponds to the HKY85 model. Under the Run Termination criteria "Bootstrap repetitions" was set to 2,000 and "Generations without improving topology" was set to 5,000 as suggested in the GARLI manual when using bootstrap repetitions. Node

confidence was scored using the bootstrap resampling method and 50% cutoff. Bayesian trees were obtained using MrBayes v3.1.2 (Ronquist and Huelsenbeck 2003) and the parallel version of MrBayes v3.1.2 (Altekar et al. 2004). MrBayes settings were as follows: 2 rate substitution model, relative rate distribution = gamma, number of generations = 1,000,000, sample freq = 1,000, number of chains = 4, and temperature = 0.2. "Burnin" was assessed using the sump command. Normally the first 1 or 2 trees were discarded as "burnin" before creating the final consensus tree. Node confidence was scored using the Bayesian posterior probability provided by the program.

Independent homeobox PCR survey supports bichir has 4 Hox clusters

Whole genomic DNA of was extracted from 80 milligrams of ethanol preserved tissue of *Polypterus senegalus* using the Dneasy kit (Qiagen) following the manufacturers' protocols. This individual is unrelated to that used for the construction of the BAC genomic library.

PCR amplification of an 81 base pair (bp) fragment of the highly conserved homeobox of PG1-8 was performed using a degenerate homebox primer pair [334, 5′-GAR YTI GAR AAR GAR TTY-3′; 335, 5′-ICK ICK RTT YTG RAA CAA-3′]. PCR amplification of an 114 bp fragment of the highly conserved homeobox of PG9–13 was performed using the degenerate primers [HB913Forward, 5′–AAA GGA TCC TGC AGA ARM GNT GYC CNT AYA SNA A–3′; HB113Reverse, 5′– ACA AGC TTG AAT TCA TNC KNC KRT TYT GRA ACC A–3′]. PCR amplifications were performed with AmpliTaq Gold DNA polymerase (Applied Biosystems) using the following cycling parameters: initial denaturation at 95 °C for 5 min, 30 cycles of 95 °C for 1 min, 50 °C for 1 min, and 72 °C for 1 min, and final extension at 72 °C for 10 min. Final concentration of $MgCl_2$ was 3.5 millimolar. Amplified fragments were purified by agarose gel extraction (Qiagen) and cloned into a pGEM-T Easy vector (Promega) following the

manufacturer's protocol. Clones containing inserts of the correct size were identified using colony PCR and sequenced (UMDNJ DNA Sequencing and Synthesis Core Facility). For each clone, both strands were sequenced using T7 and SP6 sequencing primers. Sequences have/will be deposited in GenBank (Acc. nos. XX).

The 81 bp and 114 bp long sequences of PG1-8 and PG9-13 homeoboxes, respectively, were compared with the corresponding sequence fragments from a range of chordates (see above). The membership of each PCR fragment to one of the paralog groups Hox1-Hox13 was initially determined based on nucleotide and amino acid sequence similarity to published *Hox* sequences using BLAST (Altschul et al., 1997). The second layer of analysis used neighbor-joining (Saitou and Nei, 1987) trees with deduced amino acid sequences and assigned bichir PCR fragments based on the subtree in which they are located. With the exception of the 'middle-group paralogs' Hox4-Hox7, we find that the paralog-groups are reconstructed as monophyletic clades.

Quartett mapping (Nieselt-Struwe and von Haeseler, 2001) has been shown previously to be able to resolve paralog-group membership of chordate *Hox* gene fragments produced by PCR surveys (Stadler et al., 2004; Chambers et al., 2008). We use `quartm`, our own C implementation of the method. In order to assign the middle group genes, we use the homeobox fragments from the clusters described above as well as teleost homeobix fragments compiled by Prohaska and Stadler (2004). For each of the middle group sequences, we first determine QM support for membership in paralog groups PG4, PG5, and the combination of PG6 and PG7. For those sequences that are not assigned to PG4, we repeat the analysis, this time testing for relative support of membership in PG5, PG6, and PG7.

The latest version of `quartm` implements an extension to quintuples. For each query sequence x, we check for membership in four groups *R, U, V,* and W, by computing QM support for each of the six tree topologies

(({*x*},*R*)|(*U*,(*V*,*W*))), (({x},R)|(V,(U,W))), (({x},R)|(W,(U,V))),

(({x},(R,U))|(V,W)), (({x},(R,V))|(U,W)), and (({x},(R,W))|(U,V)),

i.e., we determine which assignment of the four paralog groups to *R, U, V, W* yields the maximal support for the tree. Ideally, *x* isplaced together with the same paralog group, say *R*, three times andplaced together with the combination of *R* and one other paralog group in the remaining three quartets. We first cross-checked the assignment of the middlegroup genes using this technique. For each paralog group, we then used QM to determine membership to one of the clusters *Hox*A, *Hox*B, *Hox*C, *Hox*D. We used the simple QM procedure when known sequences from three paralog groups are available, and the quintuple version if homeboxes of all four paralog groups are known. Finally, we used QM to determine whether the bichir sequences associate with one the duplicated teleost sequences or with the unduplicated tetrapod or shark sequences.

The QM analysis was complemented by the construction of neighbor joining (Saitou and Nei, 1987} and maximum parsimony (Swofford, 2003) trees from the same datasets.

Phylogenetic footprinting analysis of chordate Hox clusters

Phylogenetic Footprint Clusters (PFCs) were obtained by searching pairwise alignments of orthologous intergenic regions using criteria outlined in (Chiu et al., 2002). PFCs in this study were further restricted to an overall 60% identity or the presence of five (5) or more individual phylogenetic footprints (PFs) (Tagle et al., 1988; Chiu et al., 2002). PFCs that corresponded to repeat- masked elements were excluded (see below, http://repeatmasker.genome.washington.edu/).

The phylogenetic footprinting method requires sufficient contrast between the foreground of functional elements and the unconstrained genomic background. Ideally, the background should be randomized. An additive divergence time of at least 250 million years is suggested for mammalian taxa (Tagle et al., 1998). To address this, we calculated *Hox* intergenic distances between different teleost fishes [*Takifugu rubripes*, Japanese pufferfish, Tru; *Tetraodon nigroviridis*, spotted-green pufferfish, Tni; *Oryzias latipes*, medaka, Ola; *Danio rerio*, zebrafish, Dre] and mammalian proxies with approximately similar divergence dates [*Homo sapiens*, human Has; *Papio hamadryas*, baboon, Pha; *Canis familiaris*, Dog, Cfa;), *Monodelphis domesticus*, opossum, Mdo] (Suppl. Figure 1). *Hox* intergenic regions (*Hox*A13-A11, *Hox*A5-A4, *Hox*B9-B8, *Hox*B3-B2, *Hox*C12-C11, *Hox*C8-C6, *Hox*D12-D11, and *Hox*D4-D3 were aligned for all species using clustalW algorithm in MacVector 9.0. Jukes-Cantor D-values were calculated from these alignments using Mega version 3.1. The saturation level of the *D* measure was determined by aligning randomly selected non-homologous intergenic regions (Suppl. Figure 1).

To obtain PFCs, pair wise alignments were made between orthologous intergenic regions of *Hox* clusters of horn shark, coelacanth, human and tetrapods, bichir, and teleosts using clustalW in MacVector 8.0. As illustrated in Suppl. Figure 2, we propose a nomenclature system for *Hox* PFCs that can accommodate the discovery of additional PFCs using the formula:

$$X = \frac{distAP}{distAB} + A$$

Let X = number of new PFC
Let P = new PFC
Let A = PFC 5' to P
Let B = PFC 3' to P

The PFCs reported here, together with any available annotation, are compiled in a Database of Gnathostome Hox PFCs, which is accessible from \TODO{\url{***}.

Cloning of PFC fragments of the Bichir and Small Linkages of the HoxC cluster

The PCR survey indicates that bichir has *Hox*C genes in its genome. Using degenerate *Hox*C4 primers, we amplified, cloned, and sequenced the *Hox*C4 ortholog in bichir (Chambers et al., 2008). The homeobox sequence of this clone is an exact match to the homebox fragment assigned as *Hox*C4 found in the PCR survey (see above). Unfortunately, PCR screening of the library pools with bichir specific *Hox*C4 primers […] and hybridization of the high density filters with the bichir *Hox*C4 probe did not yield any *Hox*C cluster containing clones.

We took advantage of our extensive *Hox* database of conserved non-coding sequences to build linkages of the *Hox*C cluster, starting with the bichir *Hox*C4 gene proper and *Hox*C13 homeobox sequences isolated in our PCR homeobox survey. We amplified and sequenced two highly conserved blocks of noncoding sequences in the bichir and then, using long PCR, made linkages to the *Hox*C4 and *Hox*C13 loci. [**NOTE: more details need here- get primers, length of PCR products, etc].**

Analysis of repetitive and mobile DNA elements in chordate Hox Clusters

Repeat Masker (RM) analysis of human, zebrafish, and pufferfish *Hox* clusters was carried out using human (*H. sapiens*), zebrafish (*D. rerio*), and pufferfish (*T. rubripes*) databases, respectively. RM analysis of frog and chick *Hox* clusters was carried out using the human database (results not shown). RM analysis of shark, coelacanth, and bichir *Hox* clusters was carried out using the human, zebrafish, and pufferfish databases. RM analysis of medaka and nile

tilapia *Hox* clusters was carried out using the zebrafish and pufferfish databases. (http://repeatmasker.genome.washington.edu/).

Excluding simple repeats, we mapped all mobile element (3 classes: DNA transposons, LTR retrotransposons, and non-LTR retrotransposons (autonomous and non-autonomous) insertions into and flanking the jawed-vertebrate *Hox* clusters. The total length in base pairs (bp) for each class of element (e.g. DNA transposons) was divided by the intergenic length (e.g. *Hox*A13-*Hox*A11) in bp to determine the relative % length. The full dataset is available at our FTP server (ftp://lifesci.rutgers.edu/chiu-review).

RESULTS

Bichir Hox Clusters

Figures 2, 3 summarize the information on the bichir *Hox* complement. In line with Chiu et al., 2004 we find that *Polypterus* has four *Hox* clusters that are orthologous to the four canonical gnathostome clusters (HoxA, B, C, D). We have identified BAC clones that contain parts of *Hox* clusters of the bichir. These cover the *Hox*A cluster, almost the complete *Hox*B cluster and two fragments of the *Hox*D cluster. The sequences are deposited in Genbank under accession numbers [].

A detailed phylogenetic analysis of full-length gene sequences was performed to confirm their identity and orthology to known *Hox* sequences. Figure 4 shows the results for *Hox*B5, *Hox*D1, and the independently cloned *Hox*C4 sequences. Interestingly, the bichir is the first actinopterygian reported to have a *Hox*D1 locus.

A PCR survey for bichir homeoboxes resulted in more than 300 clones of 27 distinct homeoboxes (Genbank accession numbers …) (Figure 3). To test the reliability of our combined Quartett-Mapping and phylogenetic analyses, we analyzed homeobox fragments independently

from the sequences identified in the BAC library screen, when available (Figure 3). In each ease, the assigned homeobox identity was identical using independent methods. The same is true for gene proper sequences of *Hox*B13, *Hox*D9, and *Hox*C4, acquired by PCR amplication of bichir whole genomic DNA (Figure 3). This lends further credibility to the identity of the remaining PCR fragments, in particular those predicted to belong to the *Hox*C cluster (for which no BAC clones were detected in this study).

Although we do not quite have a complete picture, the *Hox* gene complement of the bichir overall matches well with the inferred actinopterygian ancestor (Hoegg and Meyer, 2005; Prohaska et al., 2006). Not surprisingly, we also observe some lineage-specific gene losses: besides the *Hox*A7 pseudogene (Chiu et al., 2004) there is no evidence for a *Hox*D13 in the BAC clone of the *Hox*D cluster that contains *evx2* and *Hox*D12 (Figure 2). We also do not find a *Hox*D14 locus, as has been reported in coelacanth (Powers and Amemiya reference) and amphioxus (reference). So far, only two microRNAs have been identified: the mir-196 paralog on the *Hox*A cluster, and the mir-10 paralog on the *Hox*B cluster.

Analysis of Phylogenetic Footprint Clusters

We have created a comprehensive database of *Hox* PFCs (Appendix) with a novel nomenclature system. To create this database *Hox*A, B, C, and D clusters of cartilaginous (hornshark), lobe-finned (human, frog, chick, coelacanth), and basal ray-finned fish (bichir) and their orthologous paralogs HoxAa, Ab, Ba, Bb, Ca, Cb, Da, and Db of teleosts (zebrafish, striped bass, nile tilapia, medaka, pufferfishes) were pairwise aligned and screened for the presence of PFCs.

We define a PFC as *deeply conserved* if it is shared between at least two of the following groups: (1) horn shark, (2) more than two sarcopterygians (lobe-finned fishes), (3) bichir (4) more than two teleosts. All PFCs were blasted against the expressed sequence tag (EST) database (http://www.ncbi.nlm.nih.gov/BLAST/). If human or zebrafish contained the PFC then their sequence was preferentially used to perform the \texttt{blast} search. All PFCs were also blasted against the Genbank nr database to identify untranslated regions and microRNAs.

Figure 4 shows the deeply conserved PFCs for the four gnathostome consensus *Hox* clusters. Consistent with the deuterostome posterior flexibility hypothesis (Ferrier et al., 2000), there are considerably fewer PFCs in the 5' (posterior) end of the *Hox* cluster than in the 3' (anterior) portion. The sequences identified include several known *Hox* enhancers (references) as well as microRNAs (references) associated with the *Hox* clusters (Figure 4, black bars). Several of the deeply conserved PFCs fall in annotated UTRs (Figure 4, red bars) or in flanking sequences within 500 bp of a *Hox* coding sequence (Figure 4, blue bars). A number of additional PFCs show homology with ESTs (Figure 4, green bars) and hence are likely expressed. These may either be part of hitherto unannotated alternative forms of *Hox* genes, (Hadrys et al., 2004; Mainguy et al., 2007, Popovic et al., 2008), or belong to non-coding transcripts. Recent studies have identified a plethora of novel non-protein-coding transcript throughout *Hox* clusters, some of which have global regulatory functions within the *Hox* expression system (Kapranov et al., 2007, Mainguy et al., 2007, Petruk et al., 2007, Rinn et al., 2007, Sasaki et al., 2007, Lempradl et al., 2008, Dinger et al, 2008 [PMID:18562676]). We compared the PFCs identified here with data from two computational surveys of non-coding RNAs using RNAz, a program that identifies substitution patterns characteristic for evolutionary conserved secondary structure

(Washietl et al, 2005). Of the 236 PFCs annotated in *Fugu rubripes* (pufferfish), 19 (including 6 microRNAs) match ncRNA predictions for fugu (Rose et al., 2008). Of the 144 human PFCs, 28 (including 4 microRNAs) are ncRNA candidates according to (Washietl et al., 2005). 14 of the 135 bichir PFCs correspond to the candidates of at least one of these two screens, including two microRNAs.

There is considerable interest in the evolution of *cis*-regulatory elements in ray-finned fish *Hox* clusters (references). Due to their small size and modular nature, *cis*-regulatory elements may be a frequent target of evolution (reference) and potentially can contribute to phenotypic diversity (reference). About half of the deeply conserved PFCs found here are located outside the known *Hox* transcripts and, based on present knowledge, are non-transcribed (Figure 4, yellow bars). We consider these to be putative *cis*-regulatory sequences; these are prime candidates for experimental approaches to test their possible regulatory functions. We note that it is possible that PFCs which overlap ESTs may also have *cis*-regulatory functions. In fact, several examples of this type are known (e.g. Dlx5/6; Feng:06a).

In order to assess how ``teleost-like" the bichir *Hox* clusters are, we consider PFCs that bichir shares exclusively with non-actinopterygians, *Nb* and those that it shares exclusively with teleosts, *Nt* (Figure 5). Here we find *Nb*=17 (26%) and *Nt* =48 (74%). These numbers show a greater similarity between bichir and teleosts than earlier reported (Chiu et al., 2004). The discrepancy can be explained, however, by the much larger number of pair-wise comparisons with teleosts, which effectively increases the sensitivity for detecting bichir-teleost PFCs relative to sarcopterygians. Normalizing by the number of pairwise comparisons, the fractions of exclusively shared PFCs become almost equal. Our data therefore confirm the mosaic pattern of PFCs in the bichir *Hox*A cluster (Figure 5A).

In contrast Figure 5B illustrates that the bichir *Hox*B cluster is strikingly teleost-like: even after normalization, 80% of the PFCs are shared exclusively between bichir and teleosts. In order to check that this extreme bias is not a sampling artefact, we also counted the numbers of PFCs exclusively shared between human and other non-actinopterygians and between human and teleosts. After scaling, we find a human/non-actinopterygian association with 74% (*Hox*A) and 82% (*Hox*B). This again emphasizes the conservative nature of outgroup (i.e. non-actinoptyergian) *Hox* clusters and the plasticity of actinopterygian *Hox* clusters.

PFCs exclusive to teleosts are determined as those that are identified between zebrafish and any of the acanthomorphs, because the members of the latter clade are too closely related for phylogenetic footprinting. Again using scaled numbers, the fraction of PFCs that are teleost inventions are 49% in *Hox*Aa, 29% in *Hox*Ab, 71% in *Hox*Ba, and 44% in *Hox*Bb (Figure 5). Ignoring the 'b' paralog clusters (which due to their small number of PFCs contribute little to the overall statistics), the PFC pattern in zebrafish mirrors that of the bichir, i.e. the *Hox*Aa cluster is a mosaic of ancestral PFCs and teleost innovations, while the *Hox*Bb cluster dominated by innovations.

The origin and loss of deeply conserved PFCs can be investigated in straightforward way using parsimony to infer the edges in a simplified phylogenetic tree. Origination events are inferred at the edge leading to the last common ancestor of all taxa in which the PFC is observed; loss events map to the (edge leading to) the root of a maximal subtree in which all taxa have lost the PFC. Figure 6 summarizes the gain and loss of all *Hox*A PFCs that are represented in at least three species. For the other three clusters, PFC data for the bichir are too incomplete for a meaningful analysis.

As shown in Figure 6, there are at least 30 PFCs whose origin pre-dates the divergence of the HoxA clusters in the three major gnathostome lineages. Significant differential loss is observed, with most of these PFCs absent in the teleost *Hox*Ab cluster. Bichir does not appear to have lost any of the gnathostome or bony-fish PFCs. The teleosts, on the other hand, have lost 7 of the gnathostome PFCs and 2 of the bony-fish PFCs before the FSGD. The *Hox*Aa cluster is much more conservative than the *Hox*Ab cluster, which appears to be very degenerate in its PFC content, having lost 14 gnathostome PFCs, 1 bony-fish PFC, and 5 ray-finned fish PFCs after the FSGD. All seven actinopterygian-specific innovations pre-date the divergence of bichir and the teleosts. In contrast, teleosts did not conserve any PFCs that were gained after the divergence of bichir and teleosts. Finally, the zebrafish *Hox* clusters retain a larger number of PFCs with non-teleosts than the acanthomorphs.

Repetitive Elements

Repetitive elements are known to be dramatically depleted in the core of vertebrate *Hox* clusters compared to the regions the regions up-stream and down-stream of the cluster (Wagner et al. 2006; Stadler paper). Our results show that DNA transposons have not invaded the *Hox* clusters of shark and tetrapods (human, chick, frog) (Figure 5A) and, in general, the *Hox* clusters of these taxa have been minimally invaded by LTR and non-LTR retrotransposons. Interestingly, the human *Hox* clusters have been invaded by several *Alu* and SINE elements (pink bars, Figure 5A) and these contribute significantly to intergenic distances (e.g. between *Hox*B13 and *Hox*B9, Figure 5A). In contrast, Fig. 5A shows the *Hox* clusters of coelacanth (green bars) and especially bichir (blue bars) have been invaded by mobile elements of all three classes, the majority of which are DNA transposons. The most striking finding of this study is the dramatic expansion of the pattern already emerging in bichir of invasion of DNA transposons into duplicated *Hox*

clusters of derived teleosts (Figure 4B). Non-LTR retrotransposons also have invaded the *Hox* clusters of teleost lineages. Insertions of mobile elements show cluster and lineage specific patterns; of the latter, zebrafish and medaka have a large number of insertions while pufferfishes, with secondarily compacted genomes, do not.

DISCUSSION [***needs to be expanded upon]

Using independent strategies including BAC library screening, homeobox PCR Surveys phylogenetic analyses of full length genes, and the examination of patterns of conservation of noncoding sequences we have demonstrated that the bichir (*Polypterus senegalus*) has four *Hox* clusters that are orthologous to those of the ancestral gnathostome. Our results thus confirm the conclusion of previous work, which was based solely on a comparative analysis of the *Hox*A cluster (Chiu et al., 2004). Our data further reveal that the *Hox* gene complement of the bichir matches the expectations for a basal lineage, e.g., retention of the *Hox*D1 gene, which has been lost in all sequenced teleosts. On the other hand, there are a few lineage-specific gene losses.

Gnathostome *Hox* clusters contain a substantial number of deeply conserved noncoding sequence elements (Chiu et al., 2002, 2004; Santini et al., 2003; Prohaska et al., 2004) which we have investigated here by means of phylogenetic footprinting. This system of putative regulatory control elements shows surprisingly little variation between sharks, coelacanth, and tetrapods, while it has been heavily restructured *in* teleost genomes. Indeed, functional *cis*-regulatory elements have continually originated in teleosts, as shown for the *Hox*A2 enhancers in acanthomorph fishes (Tumpel et al., 2006). Teleosts have lost many of the deeply conserved ancestral PFCs, and acquired a large number of lineage-specific novel PFCs.

Our analysis shows that this process has started well before the FSGD. In fact, many of the innovations are specific to actinopterygians, and few if any PFCs originated between the divergence of the bichir for the other actinopterygians and the radiation of the crown teleosts in the wake of the FSGD. This is consistent with a previous analysis of the bichir *Hox*A cluster that attested a trend of mosaicism in the retention of PFCs compared to non-ray finned fish and teleosts (Chiu et al., 2004).

Taken together, the increased rate of intergenic sequence evolution, the elevated level of mobile element insertions, the loss of ancestral PFCs, and the innovation of a large number of novel PFCs implies a relaxation of evolutionary constraints in actinopterygian *Hox* clusters. This trend started already before the divergence of bichir and teleosts and has continued in linage-specific way in teleosts. It therefore appears that the FSGD is not the cause for the relaxation of constraints, on the contrary its success, eventually spawning the most diverse group of vertebrates, may well be the consequence the less rigid selection of *Hox* cluster organization at the base of the ray-finned fish clade.

Acknowledgments

This work was funded, in part, through grants from National Science Foundation (Grant MCB 0447478 to C.-h.C.), and the Bioinformatics Initiative of the Deutsche Forschungsgemeinschaft.

FIGURE LEGENDS

Figure 1. General framework of actinopterygian phylogenetic relationships as supported in recent hypotheses based on molecular data (Venkatesh et al., 2001; Inoue et al., 2003; Le et al., 2003; Kikugawa et al., 2004).

Figure 2. *Hox* clusters of the bichir (*Polypterus senegalus*).. Gene symbols indicate the evidence for its presence. Dotted outlines indicate (Hox) genes that are present in (some) teleosts but have not been identified in the bichir so far. Lines indicate linkage. The dotted line in *Hox*B and *Hox*D clusters indicates that the BAC clone sequences are not finished, full lines indicates linkage on a contig. A bullet indicates PCR clones whose assignment is corroborated by additional genomic DNA. Genes for which only PCR clones are available are shown only when their identity is strongly supported by quarttet mapping and phylogenetic analysis.

Figure 3. Gene trees of *Hox*B5 (A), *Hox*C4 (B), and *Hox*D1 (C) orthologous sequences. For each figure, the blue arrow indicates the ortholog of bichir (*Polypterus senegalus*, Pse). In Figure 2A and 2B, bichir has a single ortholog that branches prior to the duplication event that produced ‘a’ and ‘b’ paralogs in teleost fishes such as zebrafish (Dre) and fugu (Tni). In Figure 2C, bichir has a HoxD1 ortholog, the first HoxD1 ortholog discovered in the ray-finned fish clade. HoxD1 is absent in all teleost fishes examined to date and was originally hypothesized to have been lost in the actinopterygian ancestor. Tree constructed from nucleotide sequences using Bayesian methods (1000000 generations). Species abbreviations: Aca, (*Amia calva*, bowfin); Aro, (*Anguilla rostrata*, eel); Dce, (*Dorosoma cepedianum*, shad); Dre, (*Danio rerio*, zebrafish); Hal,

(*Hiodon alosoides*, goldeye); Hfr, (*Heterodontus franscisci*, horn shark); Hsa, (Homo sapiens, human); Lme, (*Latimeria menadoensis*, coelacanth); Mat, (*Megalops atlanticus*, tarpon); Ola, (*Oryzia latipes*, medaka); Omy, (*Onkorhynchus mykiss*, trout); Oni, (*Oreochromis niloticus*, tilapia); Psp, (*Polyodon spathula*, paddlefish); Sal, (*Scaphirhynchus albus*, sturgeon); Ssa, (*Salmo salar*, salmon), Tni, (*Tetraodon nigroviridis*, Spotted green pufferfish}, Tru, (*Takifugu rubripes*, Japanese pufferfish); Xla, (*Xenopus laevis*, African clawed frog); Xtr, (Xenopus tropicalis, pipid frog).

Figure 4. A map of the locations of deeply conserved phylogenetic footprint clusters (PFCs) on reconstructed gnathostome ancestor HoxA, B, C, D clusters. Black boxes denote *Hox* genes; open boxes denote *Hox* genes that are found in only a single extant gnathostome to date. Annotated elements: *Hox*C8 early enhancer (Shashikant et al., 1995), *Hox*A5 MES enhancer (Larochelle et al., 1999) , *Hox*D4 RARE (Morrison et al., 1996), *Hox*A4 RARE (Doerksen et al., 1996), *Hox*A2 enhancer (Nonchev et al., 1996), mir-196b (Yekta et al., 2004), mir-196-2 (Berezikov et al., 2005).

Figure 5. A schematic *Hox* cluster with gene content and PFC distribution. Figure 5A shows the *Hox*A clusters of human and bichir and the *Hox*Aa and *Hox*Ab clusters of zebrafish. The large pie diagram to the right of each name displays the PFC content. The numbers of PFCs were scaled based on the number of pairwise alignments performed for each category. The individual pie diagrams along the cluster describe the PFC content for each particular intergenic region. Figure 5B shows the *Hox*B cluster of human, the partial *Hox*B cluster of bichir, and the *Hox*Ba and *Hox*Bb clusters of zebrafish.

Figure 6. Gain and loss of PFCs in the gnathostome *Hox*A cluster. Solid circles denote acquisition of a new PFC in that lineage, open circles indicate losses, shown separately for acquisitions on different edges (coded by matching colors). Here we count only PFCs that are conserved between at least three species. In particular, there is no apparent gain of any PFCs at the base of the teleos clade but there is evidence of 7 new PFCs gained before the divergence of bichir at the base of the ray-finned fish clade.

Figure 7. Map of mobile element insertions into jawed vertebrate *Hox* clusters. The single *Hox* cluster of amphioxus is shown at the top with paralog groups indicated. The corresponding paralog groups are shown for *Hox* clusters of jawed vertebrates. Each jawed-vertebrate species is color coded: horn shark (red); human (pink); coelacanth (green); bichir (blue). Retention of the paralog group is indicated by presence of color corresponding to species. Rel % length (see Methods) of mobile elements detected using Repeat Masker are depicted as solid bars (DNA transposons), cross-hatched bars (LTR retrotransposons), and open bars non-LTR retrotransposons). Bars are color coded according to species.

(**A**). Map of mobile elements (shown in rel % length) invading *Hox* clusters of jawed vertebrates that retain the ancestral four clusters (A, B, C, D). Bars are color coded: red (shark), pink (human), green (coelacanth), blue (bichir).

(**B**). Map of mobile elements (shown in rel % length) invading composite duplicated *Hox* clusters of teleosts. Bars are color coded: magenta (zebrafish), green (medaka), purple (tilapia),

blue (pufferfish). *Hox* genes on ‘a’ clusters are above the line and on ‘b’ clusters are below the line.

Suppl. Figure 1. Divergence of intergenic sequences measured as Jukes-Cantor D values for pairs of teleosts and mammals, respectively that have comparable estimated dates of divergence (Benton, 2005). Selected IGRs are 1=*Hox*A13-*Hox*A11; 2= *Hox*A5-*Hox*A4; 3=*HoxB*9-*Hox*B8; 4=*Hox*B3-*Hox*B2; 5=*Hox*C12-*Hox*C11; 6-*Hox*C8-*Hox*C6; 7=*Hox*D12-*Hox*D11; 8=*Hox*D4-*Hox*D3. The green line indicates the saturation level (with error-bar) for alignments of random IGRs. Lme, *Latimeria menadoensis*; Mdo, *Monodelphis domestica*; Ola, *Oryzias latipes*; Pha, *Papio hamadryas*; Tni, *Tetraodon nigroviridus*; Tru, *Takifugu rubripes*.

Suppl. Figure 2. Proposed nomenclature for naming phylogenetic footprint clusters. The name consists of a 3-letter abbreviation for the species consisting of the first letter of the genus and first two letters of the species. A capital letter representing the Hox cluster, two subscript capital letters represent the position along the cluster, an identification number specific for each PFC, and 1-6 lower case subscript letters representing the section content of that species.

Raincrow et al., Figure 1

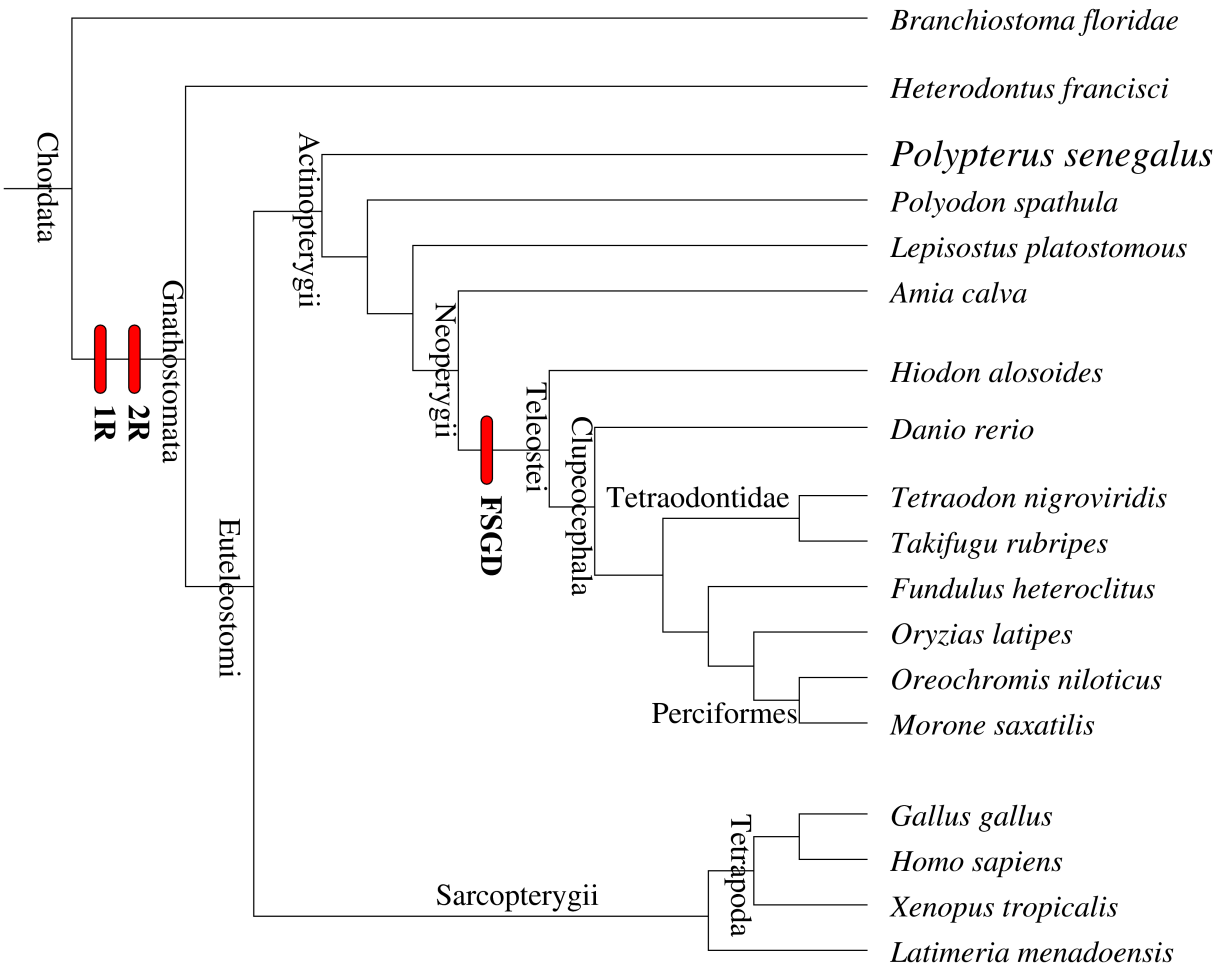

Raincrow et al., Figure 2

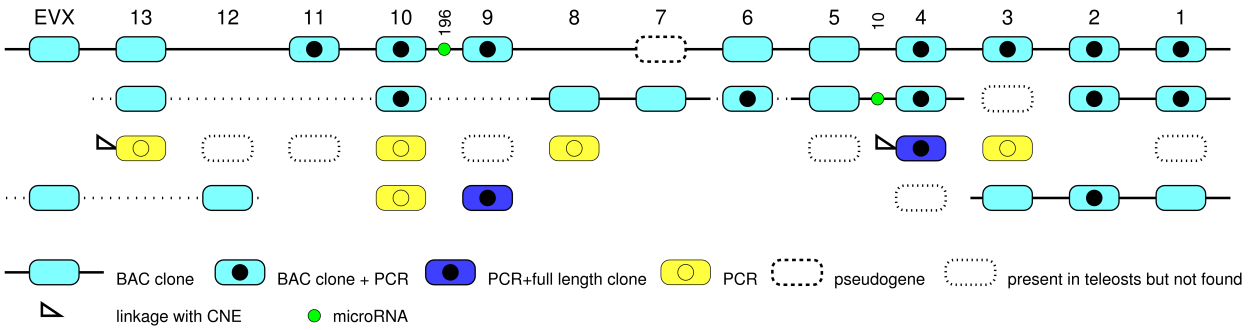

Raincrow et al., Figure 3

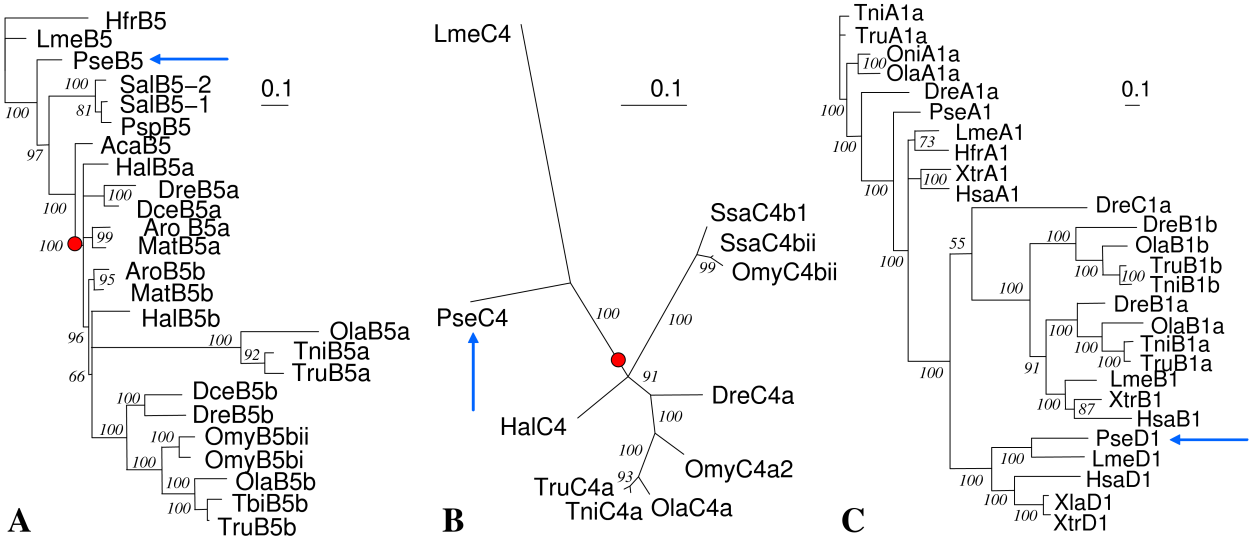

Raincrow et al., Figure 4

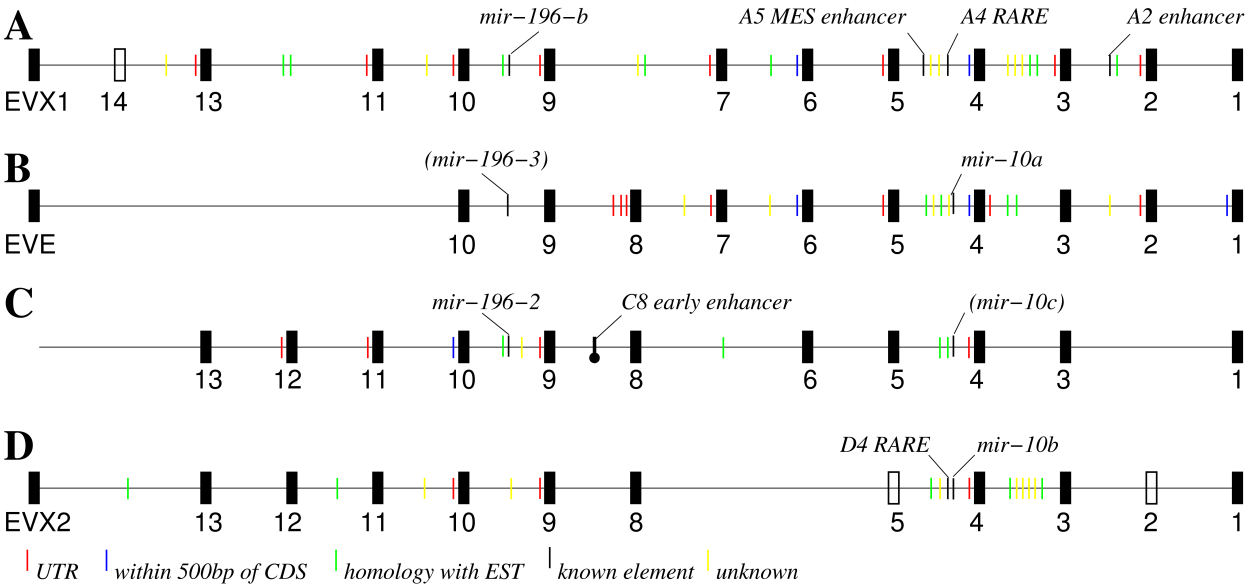

Raincrow et al., Figure 5a

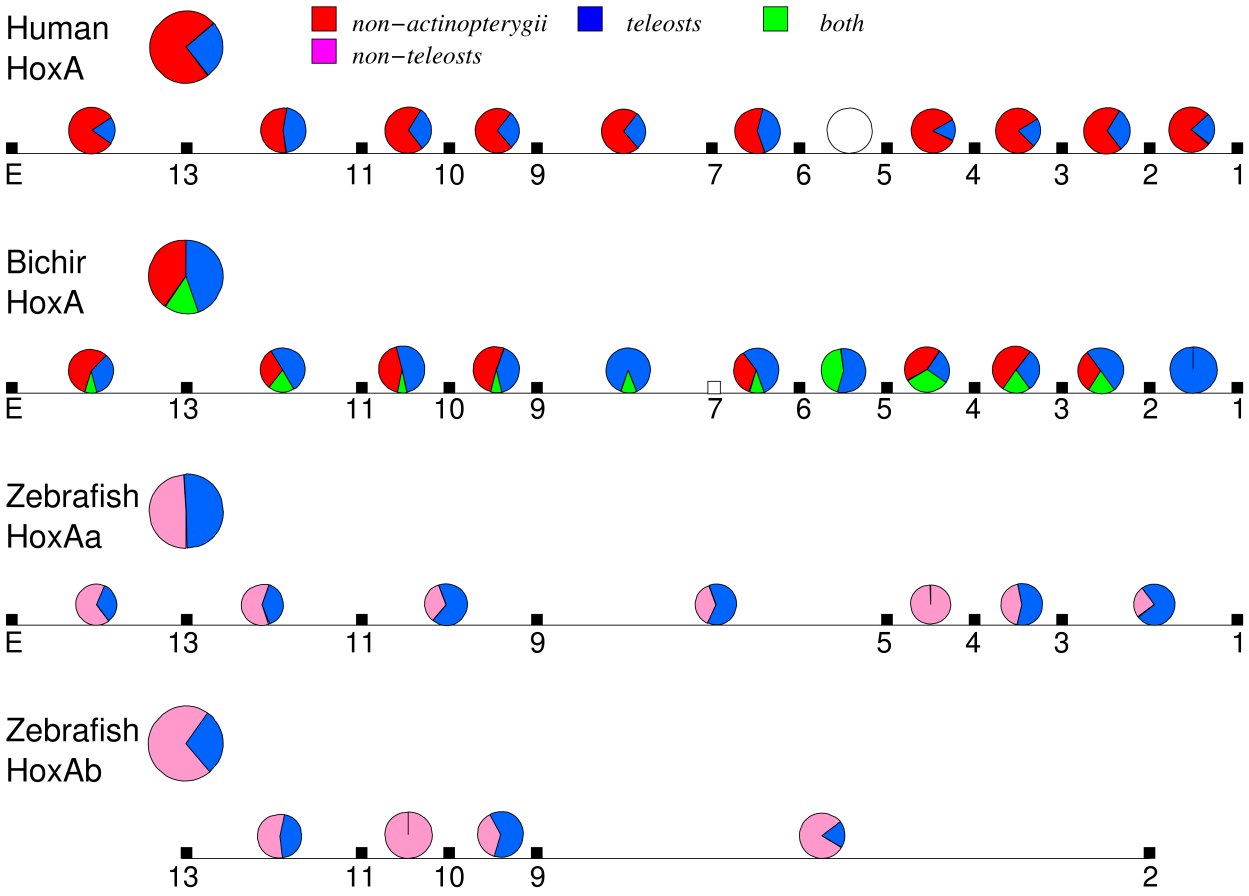

Raincrow et al., Figure 5b

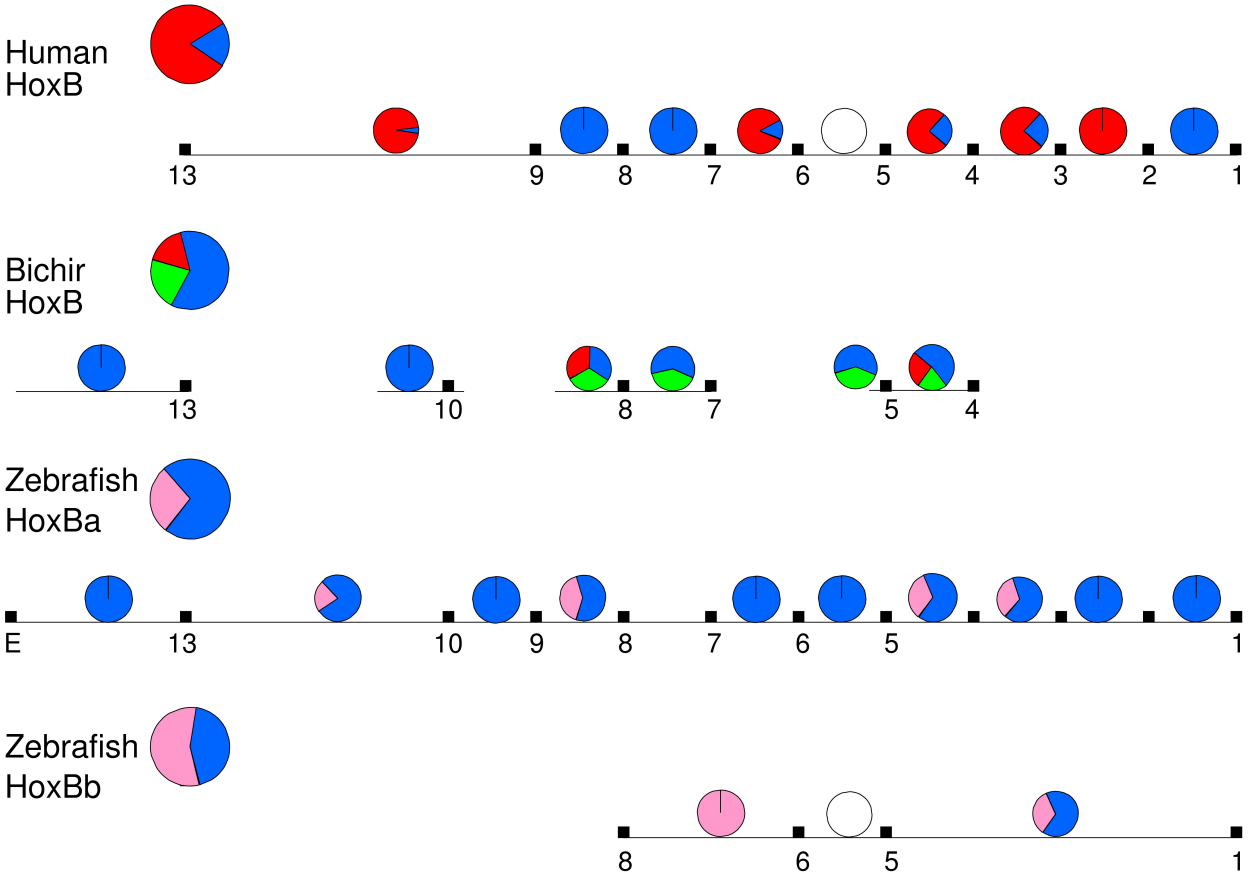

Raincrow et al., Figure 6

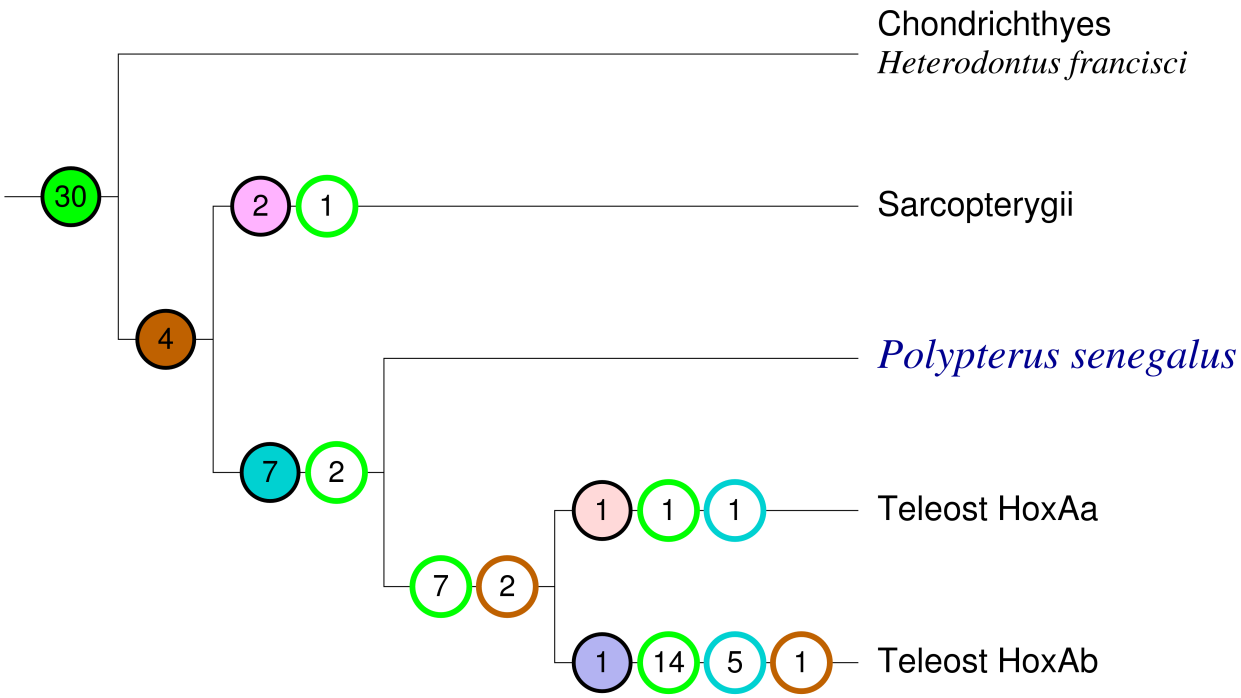

Raincrow et al., Figure 7

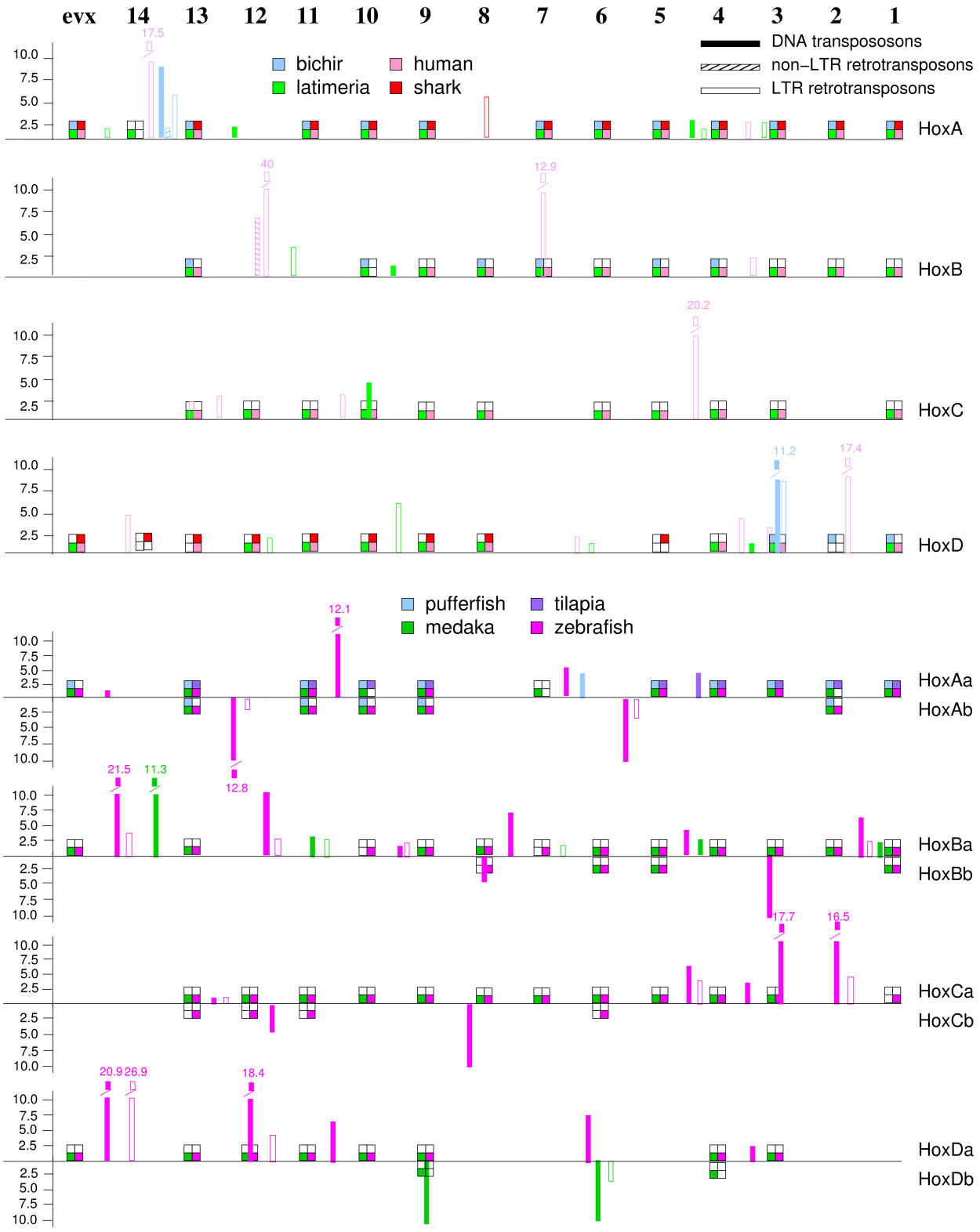

Raincrow et al., Supplemental Figure 1

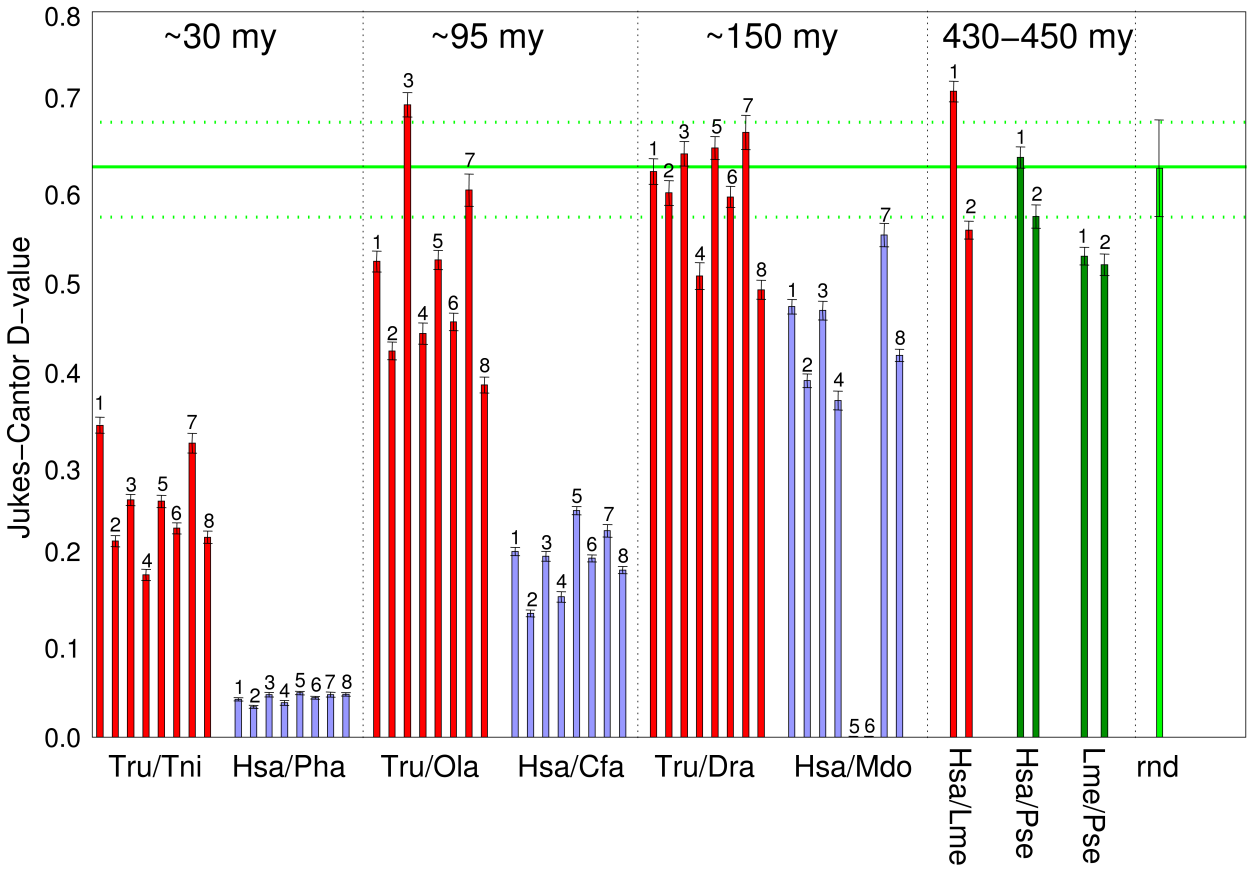

Raincrow et al., Supplemental Figure 2